

## P11.6

# THE ROLE OF ENVIRONMENTAL AND COMPUTATIONAL PARAMETERS IN THE DEVELOPMENT AND IMPACT OF THE FORWARD-FLANK GUST FRONT IN SUPERCELL THUNDERSTORMS

Jeffrey Beck\*, Christopher Weiss  
Texas Tech University, Lubbock, TX

## 1. INTRODUCTION

Conceptual understanding of the forward-flank region of a supercell thunderstorm has remained relatively unchanged over the past 20 years. Hazards associated with in-situ data collection in the forward-flank and the limited number of high resolution dual-Doppler studies of supercell thunderstorms have minimized scientific advances (Wakimoto 2002; Shabbott and Markowski 2006). Therefore, most of our understanding of the forward-flank has been gained through numerical model simulations. Yet, many of these modeling studies have shown that a product of the forward-flank, the forward-flank gust front (FFGF), may play an integral role in the production of the low-level mesocyclone. However, some dual-Doppler studies have raised questions regarding the strength and even existence of a FFGF. In light of these findings, there is a need for further research regarding the forward flank, and specifically the FFGF, in order to solidify the dynamics involved in the development of low-level vertical vorticity within supercell thunderstorms.

## 2. LITERATURE REVIEW

Perplexing and sometimes contradictory findings concerning the FFGF have existed since early supercell conceptual models. For instance, dual-Doppler research conducted by Brandes (1977, 1978, 1981, and 1984a,b) showed that not every supercell contains a kinematic FFGF. In addition, the conceptual model from Brandes (1978) (Fig. 1a) indicates a FFGF position that does not match a later model put forth by Lemon and Doswell (1979) (Fig. 1b).

More recent observational dual-Doppler studies, including Dowell and Bluestein (2002a,b) and Beck et al. (2006) have found that the FFGF was almost nonexistent in their respectively sampled storms. However, Beck et al. (2006) found that an intriguing FFGF existed aloft, with an orientation identical to that found in Lemon and Doswell (1979). In addition, the convergence associated with this FFGF increased in magnitude with height, leading the authors to speculate that forcing for the feature might have been solely kinematic

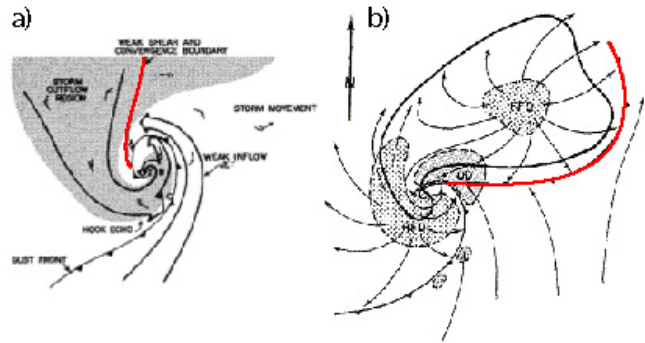


Figure 1: (a) Lemon and Doswell (1979) and (b) Brandes (1978) supercell conceptual models. FFGF indicated by red line.

in nature. Origins of potential forcing included an anticyclonic circulation aloft, combined with veering inflow winds, both of which increased in intensity with height. Dowell and Bluestein (2002a,b) also described a more traditional near-ground FFGF as mainly kinematic in nature, due to a lack of a thermodynamic gradient when sampled by mobile mesonets in the area. On the other hand, Brandes (1984b) conducted a buoyancy retrieval and found that for one storm, a radar-derived buoyancy gradient existed where the FFGF was expected to reside, but no kinematic feature (namely convergence) was present.

Two ground breaking modeling papers addressing the FFGF and its impact on vertical vorticity were Klemp and Rotunno (1983) and Rotunno and Klemp (1985). Simulations of a supercell thunderstorm showed that baroclinity along the FFGF was sufficient to produce horizontal vorticity comparable to that contained within the inflow air. This horizontal vorticity was then tilted and stretched by the updraft, forming the low-level mesocyclone. Results from subsequent modeling studies by Wicker and Wilhelmson (1995) and Adlerman et al. (1999) were in general agreement with the earlier two studies, highlighting trajectories through the region of the FFGF, terminating in the low-level mesocyclone.

It should be noted that the modeling studies defined the gust fronts thermodynamically, using the -1K perturbation potential temperature contour. The modeling studies generally found the FFGF portion of this contour oriented in a north/south fashion to the north of the mesocyclone. However, at times, the -1K perturbation

\*Corresponding Author Address: Jeffrey Beck, Texas Tech Univ., Atmospheric Science Group, Lubbock, TX 79409-2101  
j.beck@ttu.edu

potential temperature was well away from the strong thermodynamic gradient north of the mesocyclone, as in Adlerman et al. (1999).

When comparing previous research, it becomes apparent that a convention for how to define the FFGF is lacking. The observational studies have defined it largely by kinematic properties (convergence and wind shifts), while the modeling studies have used thermodynamic properties. In addition, it is not clear that use of the -1K perturbation potential temperature contour always captures what is thought to be the traditional thermodynamic FFGF. Perhaps a convention using a stronger gradient may be necessary; perhaps multiple FFGFs may exist. This ambiguity in definition, physical characteristics, and even existence is the main impetus for the research to be outlined in the following section.

### 3. METHODS AND ANALYSIS

#### 3.1. EXPERIMENTAL DESIGN

In an attempt to provide a more concise definition for the FFGF and to assess its impact on vertical vorticity, the proposed research will examine how environmental as well as computational parameters affect the FFGF. Specifically, a sensitivity modeling study will be conducted using the Weather Research and Forecasting (WRF) model.

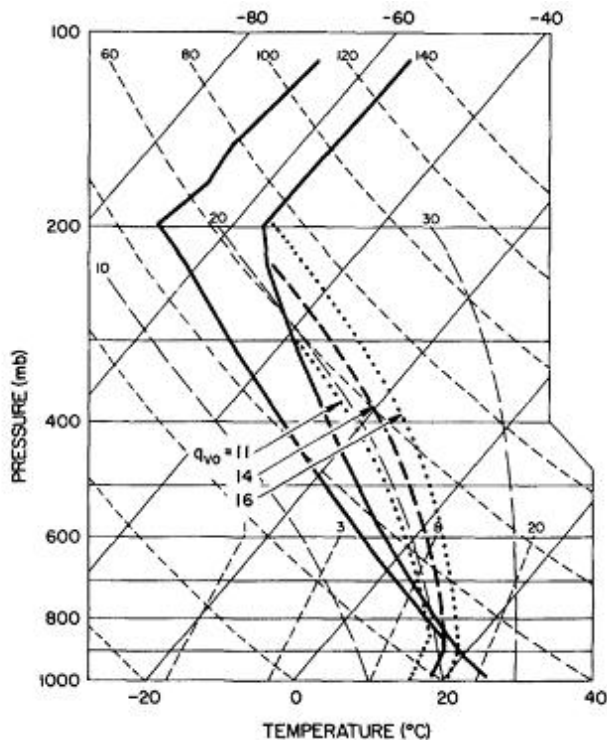


Figure 2: Idealized sounding from Weisman and Klemp (1982)

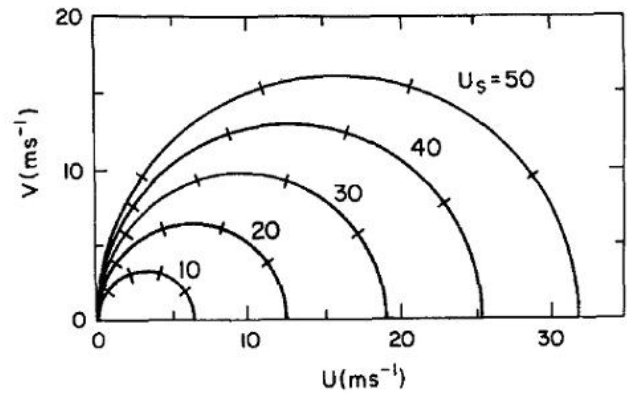


Figure 3: Idealized half-circle hodographs from Weisman and Klemp (1984).  $U_s$  is defined as the magnitude of the velocity variation along the hodograph curve.

A control simulation will be conducted using the smoothed idealized sounding (Fig. 2) and hodograph ( $U_s=50 \text{ ms}^{-1}$ ) (Fig. 3) from Weisman and Klemp (1982, 1984) in an attempt to roughly approximate the 20 May 1977 Del City, OK composite sounding and hodograph used in the modeling studies discussed previously. The details of the control simulation are outlined below:

Coarse grid dimensions	100 x 100 x 43 (50 km x 50 km x 15 km)
Fine grid dimensions	120 x 120 x 43 (20 km x 20 km x 15 km)
Horizontal grid spacing	500 m (coarse), 167 m (nest)
Vertical grid spacing	Stretched/Hyperbolic tangent (min = 100 m, max = 500 m)
Initialization	Single sounding (Weisman and Klemp, 1984)
Microphysics	WRF Single Moment 6-Class (WSM6)
Initial convective perturbation	4K thermal, Hor. Radius = 9 km, Vert. Radius = 1.5 km, Center = 1.5 km AGL

Table 1: Sensitivity Study Model Specifications

A number of recent studies, including Adlerman and Droegemeier (2002) and Bryan et al. (2003), have shown the importance of using high spatial resolution to accurately resolve specific dynamics involved in convective modeling. Therefore, in order to minimize the necessary computing power, the control simulation will consist of two nested two-way grids. The larger, coarse grid will be used primarily to define boundary conditions for the nested domain, while the fine grid will encompass a majority of the storm and will be the source of all analyzed data (similar to that done in Adlerman and Droegemeier 2000).

In order to implement the sensitivity study, a number of parameters thought to influence the development

and characteristics of the FFGF were chosen. These parameters will be altered incrementally, with one increment consisting of one model simulation. The total number of model runs will be equal to the number of parameters multiplied by the number of increments. The following is a list of these parameters and their corresponding delineations:

Parameter	Sensitivity Increment (Iterations x Increment, if applicable)
Sub-cloud specific humidity	$5 \times 2 \text{ gkg}^{-1}$
Magnitude of velocity variation	$5 \times U_s = 5 \text{ ms}^{-1}$ for both half-circle and straight-line hodographs
Cloud depth lapse rates	$5 \times 2^\circ\text{C}$ (for lowest pressure level of specific lapse rate, then linear connection)
Cloud depth specific humidity	$5 \times 2^\circ\text{C}$ (dewpoint)
Drop size distribution	Alteration of $\alpha_0 e^{-x}$ function
Horizontal resolution	100 m, 167 m, 500 m, 1.0 km, 1.5 km
Vertical resolution	Hyperbolic tangent minimum grid spacing of 50, 100, 150, 300, 500 m

Table 2: Parameters and their respective increments to be used in the sensitivity study

Two of the parameters will be segmented into smaller parts in order to assess changes on a finer scale. Specifically, portions of each hodograph (0-1 km, 0-3 km, 0-6 km, and 6-15 km AGL) as well as the cloud depth lapse rate (LCL-600 mb, 600 mb-400 mb, and 400-200 mb) will be examined separately, in addition to each full hodograph and LCL-EL lapse rate.

For each parameter there are five increments, one as the control simulation, with four other increments, potentially split about the control value, or some other variation. For example, the control value of horizontal resolution is 167 m. There will be three increments larger than this value (500 m, 1.0 km, and 1.5 km) and one increment less than the control value (100 m).

### 3.2. STATISTICAL ANALYSIS

In order to examine the impact of each parameter (predictor variable) selected in Table 2, it is necessary to collect data relevant to the FFGF from each simulation. Once collected, linear regression can be conducted to analyze the sensitivity of FFGF characteristics based on the predictor variables. Therefore, Table 3 outlines the regressor parameters to be collected from each simulation, along with other pertinent information.

The collection of these regressor variables will be undertaken at both 100 m and 1.5 km AGL, within a 5 km radius west through east (via north) of the mesocyclone, when the mesocyclone vertical vorticity is at a maximum for each simulation at 1 km AGL. Two levels

Regressor	Height of Collection	Association with FFGF
Maximum near-ground convergence	100 m and 1.5 km AGL	Defining kinematic characteristic of FFGF
Maximum near-ground horizontal vorticity	100 m and 1.5 km AGL	Total baroclinic and barotropic production of horizontal vorticity
Orientation of FFGF (thermo/kinematic)	100 m and 1.5 km AGL	Potential trajectory impact
Maximum near-ground buoyancy gradient	100 m and 1.5 km AGL	Solenoidal/baroclinic production of horizontal vorticity
Maximum vertical vorticity of mid-level anticyclone	Varies on a case by case basis	Kinematically produced convergence/horizontal vorticity aloft

Table 3: Summary of regressor variables directly associated with the FFGF

will be assessed since trajectory analyses from previous research showed that many parcels terminating in the low-level mesocyclone have origins at multiple levels (e.g., Wicker and Wilhelmson (1995)). In addition, Beck et al. (2006) showed that a FFGF may exist aloft, but not near the surface.

In addition to these regressors, which are all related to the FFGF and associated horizontal vorticity, a separate regression analysis will be conducted on parameters associated with the low- and mid-level vertical vorticity. Therefore, these regressors (maximum value of vertical vorticity) will be collected at 1.0 km AGL and 6 km AGL, respectively. This separate regression analysis will allow for the comparison of sensitivity effects on both horizontal vorticity (FFGF) and then vertical (mesocyclonic) vorticity. If the regression analyses are similar, this may suggest that FFGF horizontal vorticity is indeed being tilted and stretched by the updraft. This supposition will be tested with the trajectory analysis.

### 4. TRAJECTORY ANALYSIS

The second part of the sensitivity study involves a trajectory analysis of parcels entering the low-level mesocyclone. The simulations with minimum, median, and maximum values of the predictor variables will be chosen for trajectory analysis and will be assessed when the low-level vertical vorticity at 1 km AGL is highest for each parameter. This sampling should provide a sufficient array of potential outcomes at the peak of low-level vertical vorticity. Specifically, parcels surrounding the perimeter of the low-level mesocyclone (1 km AGL) will be chosen as ultimate locations for the trajectories.

Trajectories provide important information concerning the thermodynamic and kinematic properties of parcels due to interactions with different portions of the storm. Assessment of parcel characteristics along tra-

jectory paths will be undertaken via vorticity and buoyancy tendency analyses. Evaluation of parcel trajectories will offer insight about source regions for vertical vorticity as well as an opportunity to assess the importance of the FFGF and any potential temperature gradient which may exist along the forward-flank reflectivity gradient. Assessment of the importance of the FFGF through trajectory analyses implies that the orientation of at least a portion of the FFGF is aligned with trajectory paths. Therefore, analysis of trajectories will also reveal the importance of this orientation.

In addition, the trajectory analysis will be used as verification of the comparison between the vertical vorticity and FFGF sensitivity studies. If the regression equations are similar, the trajectory analysis should confirm the similarity by showing parcel residence time within some portion of the FFGF before reaching the low-level mesocyclone during the peak in vertical vorticity.

## 5. CONCLUSIONS AND FUTURE WORK

Past modeling research has indicated a potentially substantial role for the FFGF in the development of vertical vorticity within a supercell thunderstorm. However, highlighted by some observational studies, ambiguity regarding the formation, structure, and therefore impact of the FFGF still exists. Therefore, the goal of this research is to gain a better understanding for the environmental and computational parameters that are important in the formation of the FFGF. To meet this end, a model sensitivity study will be conducted, followed by linear regression using selected parameters thought to influence the development and structure of the FFGF. In addition, trajectory analyses will be combined with the regression to assess the impact of the FFGF on vertical vorticity within the storm. Future research will involve verification of the sensitivity study through WRF model data assimilation. Observational supercell datasets collected during field projects by mobile Doppler radar, mobile mesonets, and the Texas Tech University StickNet will provide the basis of this future work. Using the regression models, predictions can be made for FFGF characteristics given the environmental parameters used as initialization for the model. Verification can then be assessed by analyzing the formation, structure, and impact of the FFGF in the observed storm. Validation of the regression models would be a positive step toward a better understanding of the FFGF.

## ACKNOWLEDGEMENTS

This research is supported by the Wind Science and Engineering Research Center at Texas Tech University. Thanks are due to both Drs. David Dowell and

John Schroeder for their valuable input regarding this research.

## REFERENCES

- Adlerman, E.J., and K.K. Droegemeier, 2000: A numerical simulation of cyclic tornadogenesis. Preprints, 20th Conference on Severe Local Storms, Amer. Meteor. Soc., Orlando, FL.
- , and K. K. Droegemeier, 2002: The sensitivity of numerically simulated cyclic mesocyclogenesis to variations in model physical and computational parameters. *Mon. Wea. Rev.*, 130, 2671-2691.
- , K. K. Droegemeier, and R. Davies-Jones, 1999: A numerical simulation of cyclic mesocyclogenesis. *J. Atmos. Sci.*, 56, 2045-2069.
- Beck, J. R., J. L. Schroeder, and J. Wurman, 2006: High-resolution dual-Doppler analyses of the 29 May 2001 Kress, Texas, cyclic supercell. *Mon. Wea. Rev.*, TBA, TBA.
- Brandes, E. A., 1977: Gust front evolution and tornado genesis as viewed by Doppler radar. *J. Appl. Meteor.*, 16, 333-338.
- , 1978: Mesocyclone evolution and tornadogenesis: Some observations. *Mon. Wea. Rev.*, 106, 995-1011.
- , 1981: Finestructure of the Del City-Edmond tornadic mesocirculation. *Mon. Wea. Rev.*, 109, 635-647.
- , 1984a: Relationships between radar derived thermodynamic variables and tornadogenesis. *Mon. Wea. Rev.*, 112, 1033-1052.
- , 1984b: Vertical vorticity generation and mesocyclone sustenance in tornadic thunderstorms: The observational evidence. *Mon. Wea. Rev.*, 112, 2253-2269.
- Bryan, G. H., J. C. Wyngaard, and J. M. Fritsch, 2003: Resolution requirements for the simulation of deep moist convection. *Mon. Wea. Rev.*, 131, 2394-2416.
- Dowell, D. C., and H. B. Bluestein, 2002a: The 8 June 1995 McLean, Texas, storm. Part I: Observations of cyclic tornadogenesis. *Mon. Wea. Rev.*, 130, 2626-2648.
- , and H. B. Bluestein, 2002b: The 8 June 1995 McLean, Texas, storm. Part II: Observations of cyclic tornadogenesis. *Mon. Wea. Rev.*, 130, 2649-2670.
- Klemp, J. B., and R. Rotunno, 1983: A study of the tornadic region within a supercell. *J. Atmos. Sci.*, 40, 359-377.
- Lemon, L. R., and C. A. Doswell, 1979: Severe thunderstorm evolution and mesocyclone structure as related to tornadogenesis. *Mon. Wea. Rev.*, 107, 1184-1197.
- Rotunno, R., and J. B. Klemp, 1985: On the rotation and propagation of simulated supercell thunderstorms. *J. Atmos. Sci.*, 42, 271-292.
- Shabbott, C. J., and P. M. Markowski, 2006: Surface in situ observations within the forward-flank downdrafts of supercell thunderstorms. *Mon. Wea. Rev.*, 134, 1422-1441.
- Wakimoto, R. M., 2002: Convectively driven high wind events. Severe Convective Storms, Meteor. Monogr., No. 50, Amer. Meteor. Soc., 255-298.

Weisman, M. L., and J.B. Klemp, 1982: The dependence of numerically simulated convective storms on vertical wind shear and buoyancy. *Mon. Wea. Rev.*, 110, 504-520.

———, and J.B. Klemp, 1984: The structure and classification of numerically simulated convective storms in directionally varying wind shears. *Mon. Wea. Rev.*, 112, 2479-2498.

Wicker, L. J., and R. B. Wilhelmson, 1995: Simulation and analysis of tornado development and decay within a three-dimensional supercell thunderstorm. *J. Atmos. Sci.*, 52, 2675-2703.